Bull. Mater. Sci. (2024)47:142
https://doi.org/10.1007/s12034-024-03203-6

Combined effect of graphene oxide and fly ash on behaviour of high-strength concrete: experimental and numerical investigation

P V R K REDDY[1,*] and D RAVI PRASAD[2]

[1]Civil Engineering Department, Anil Neerukonda Institute of Technology and Sciences, Visakhapatnam 531163, India
[2]Civil Engineering Department, National Institute of Technology, Warangal 506004, India
*Author for correspondence (pvrkreddy20@gmail.com; pvrkreddy.ce@anits.edu.in).

MS received 3 November 2023; accepted 3 January 2024

Abstract. Graphene oxide (GO) is a potential material for application as nano-reinforcements in cementitious composites owing to its high-water dispersibility, aspect ratio and outstanding mechanical characteristics. In this study, the combined effect of GO and fly ash on strength properties, stress–strain behaviour and static modulus of elasticity of high-strength concrete was investigated. In addition, microstructure has been characterized using SEM and EDS techniques. The addition of GO at 0.15% and the replacement of cement with fly ash at 10, 20 and 30% by weight was considered. The results exhibited that the addition of GO at 0.15% improved the compressive and flexural strength of concrete by 24.3 and 25.2%, respectively, at 7 days. The combined effect of GO and fly ash on the strength properties of concrete at 7 days was greater than control concrete demonstrating that GO can offset the effect of fly ash on delaying the strength growth at an early age. From the experimental results, it can be concluded that the addition of GO and fly ash into the concrete improved both the strength and elastic modulus, consequently exhibiting positive synergy in hybridizing GO and fly ash into the concrete. Also, the microstructure properties indicated that the GO and fly ash-based concrete mixes exhibited a denser microstructure. Furthermore, a nonlinear numerical model was also created for GO and fly ash-based concrete with finite element-based software ATENA-GiD to validate the experimental findings. The nonlinear numerical model successfully predicted the behaviour under monotonic axial compression and was quite beneficial in minimizing the tedious experimental testing. Finally, it is found that the findings of both the experimental and numerical investigations are in good agreement.

Keywords. Concrete; graphene oxide; fly ash; stress–strain relationship; strength; FEM model.

1. Introduction

Cement concrete is extensively used in civil infrastructure around the world. Progress in the field of nanotechnology has resulted in nanosized particles and fibres (e.g., carbon nanotubes and nano-silica), which may be utilized as reinforcements to further enhance the performance of cement composites. Nano-reinforcements in cement composites became more beneficial than traditional steel bars or fibre reinforcements (at the millimetre level) due to their ability to regulate nano-sized cracks (at the inception phase) prior to their progress into micro-size [1]. For instance, the incorporation of nano-silica into cement composite has been found to progress its mechanical performance [2]. The spherical shape of nano-silica with a low aspect ratio has less than 30 nm diameters and 300 $m^2\ g^{-1}$ specific surface area [3]. Two characteristics are commonly ascribed to better mechanical performances [4]. First, owing to their large specific surface area, nano-silica can act as cement phase nuclei and accelerate the hydration process. Second, due to its similar size to a gel pore in a cement matrix, nano-silica can be used as a filler to significantly densify the microstructure. However, because of its small aspect ratio, nano-silica is unable to stop the growth of microcracks that are caused by nano-size cracks, which reduces its effectiveness as a reinforcement.

Carbon nanotubes (CNTs) are one-dimensional tubes having a high aspect ratio in comparison to the spherical shape of nano-silica. It contains diameters ranging from 1–3 nm for single-walled CNTs to 5–50 nm for multi-walled CNTs [5]. CNTs can have lengths of up to centimetres, resulting in an aspect ratio greater than a thousand. CNTs are also extremely strong, with elastic modulus in the range of TPa and tensile strength in the GPa range [6]. CNTs were reported to enhance the elastic modulus [7] and strength [8] of cement composites on account of their high aspect ratio and outstanding mechanical performances. Furthermore, the inclusion of CNTs in cement composites has shown to be highly complicated, with sometimes contradictory results. A few investigations reported that adding CNTs leads to minor variation in strength, or even a decrease in strength in certain circumstances [9]. The

Published online: 08 July 2024

factors are often related to inadequate dispersion and weak connection between the cement system and the CNTs. CNTs produce agglomerates or bundles because of high Van der Waal interactions among particles, which can become defective sites in the matrix. When dispersion chemicals were employed, however, the mechanical characteristics of the composites containing CNTs improved. Apart from poor dispersion, another issue limiting its performance in cementitious materials is the problem of generating significant CNT–matrix interaction. It is comparable with a graphene sheet that has been wrapped into a tubular form. Because the external CNTs shield the inside tubes from the matrix, the tube-shaped CNTs minimize the interfacial bonding [10].

Graphene, like CNTs, is made up of sp^2-bonded carbon atoms [11], which gives it outstanding mechanical characteristics. The modulus of elasticity and characteristic strength range around 1 TPa and 60 to 130 GPa, respectively [12]. Furthermore, a single-layer graphene sheet's aspect ratio and surface area can exceed 2000 and 2600 $m^2\ g^{-1}$, respectively, both are significantly greater than that of CNTs [13]. Nevertheless, the difficulty in dispersion of graphene and the expensive cost of manufacture prevents their potential applications. Graphene oxide (GO) is a graphene derivative which consists of a single layer of sp^2-hybridized carbon atoms functionalized with the combination of carbonyl, carboxyl and hydroxyl groups [14]. The oxygenated functionalities, which are connected to the edges and basal planes of GO sheets, considerably modify their Van der Waals bonds among the GO sheets, and improve in dispersal capability in aqueous solution [15–17]. In the cement matrix, GO was reported to have been dispersed uniformly in recent research [18]. Aspect ratio, surface area and tensile strength are other characteristics of GO that are also highly significant [19,20]. Furthermore, GO may be effectively produced from natural graphite flakes (a low-cost resource) through intense oxidation followed by exfoliation. GO is a promising nanomaterial for increasing the mechanical characteristics of cement composites because of its superior mechanical characteristics, high dispersibility in water and low-cost production. In terms of GO surface functionality, the oxygenated functionalities may further facilitate the use of these carbon nanostructures in cement composites since they develop covalent connections with hydrated phases. For instance, it is reported that carboxyl acid functions can develop a strong covalent connection with calcium silicate hydrate (C–S–H), significantly enhancing the mechanical characteristics of cement composites [21,22].

Although GO has been extensively investigated in cement paste and cement mortar, its applications in cement concrete have remained limited. According to a recent investigation of the GO–cement concretes [23–27], the incorporation of GO in the cement concrete leads to improved microstructure, resulting in increased strength characteristics compared to control concrete. However, the combined effect of GO and fly ash on the strength properties and stress–strain relationship of the concrete has not been studied. The primary objective of this study is to investigate the combined effect of GO and fly ash on the strength characteristics, stress–strain behaviour and static modulus of elasticity of high-strength concrete with characteristics compressive strength of 60 MPa. The findings of the cement composite are compared with the control concrete. Also, the microstructure of concrete has been characterized using SEM and EDS techniques. In addition, the nonlinear finite element model (FEM) was developed with finite element-based software ATENA-GiD to simulate the uniaxial compression and flexural behaviour.

2. Experimental

2.1 *Materials*

Materials employed in this experimental study are ordinary Portland cement (OPC) of 53 grade in compliance with IS:269-2015, fly ash of Class F in compliance with IS:3812 (Part 1)-2013, sand and coarse aggregates (CA) in compliance with IS:383-2016, and polycarboxylate superplasticizer (PCE) conforming to IS:9103-2018.

The physical properties of industrial-grade nanomaterial GO are given in table 1. To disperse GO in water, ultrasonication process was employed, and as a result solution at 4 $g\ l^{-1}$ concentration was achieved. SEM, EDX, FTIR and XRD tests were employed to characterize GO, as shown in figures 1, 2, 3 and 4. It can be observed from the SEM image of GO in figure 1, the morphology of GO surface is folded and wrinkled. Elemental composition in figure 2 demonstrated that GO is composed of 74.43% C, 25.04% O and 0.51% S. The XRD pattern in figure 3 indicates that the diffraction peak is present at $2\theta = 12.6°$ with an interplanar distance of 0.702 nm. The FTIR spectra in figure 4 reveal the presence of oxygen functionalities on the GO surface.

2.2 *Mix proportioning and preparation of samples*

The concrete mix with a characteristic compressive strength of 60 MPa was designed according to the IS:10262-2019 and is considered as control concrete (CC) for reference. The water-to-binder ratio was taken as 0.30 for all mixes. GO addition to the concrete mixes was in the dosage of 0.15%. The cement replacement with fly ash at a percentage of 10, 20 and 30 by weight was considered in this investigation. Mix proportions of concrete are given in table 2. The specimen preparation procedure for all mixes is similar. The cement, fly ash, sand, coarse aggregates, water and GO solution were thoroughly mixed in a mixer for 4 to 5 min to obtain a homogeneous mixture. The fresh concrete mix was

Table 1. Physical properties of GO.

Number of layers	Purity	Average lateral dimension	Thickness	Surface area	Bulk density
1–4	~99%	~5–10 μm	~0.8–2 nm	110–250 m^2 g^{-1}	0.123 g cm^{-3}

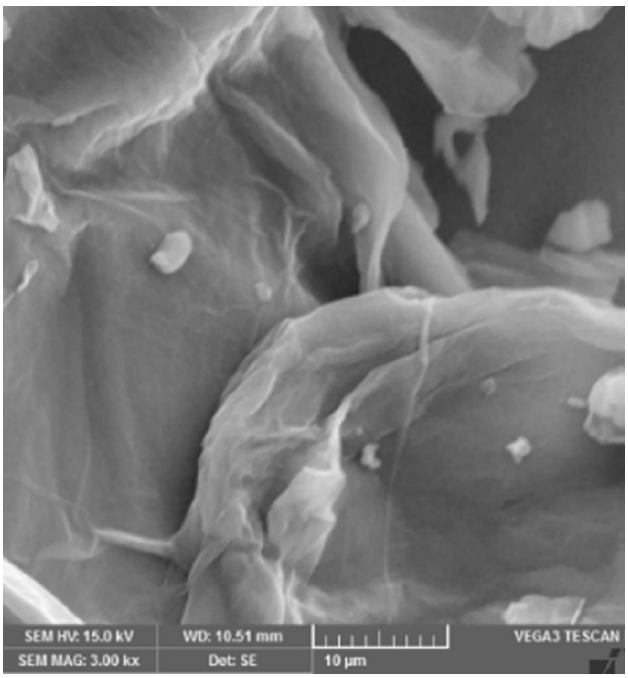

Figure 1. GO characterized by SEM.

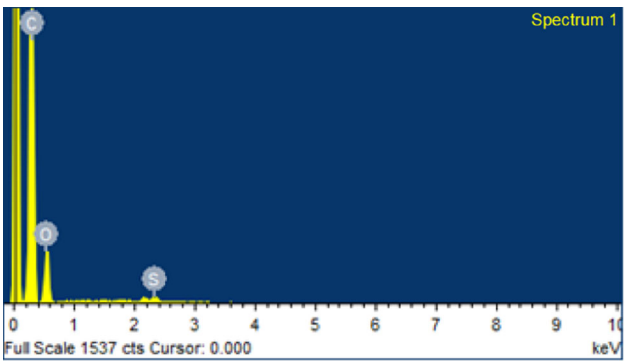

Figure 2. GO characterized using EDX analysis.

then placed into an oiled mould and vibrated on a vibration table for 15–30 s. After 24 h, the hardened concrete specimens were separated from the mould and placed in water for curing.

2.3 *Compressive strength*

Compressive strength test is carried out on a cylindrical specimen of size 100 × 200 mm according to ASTM

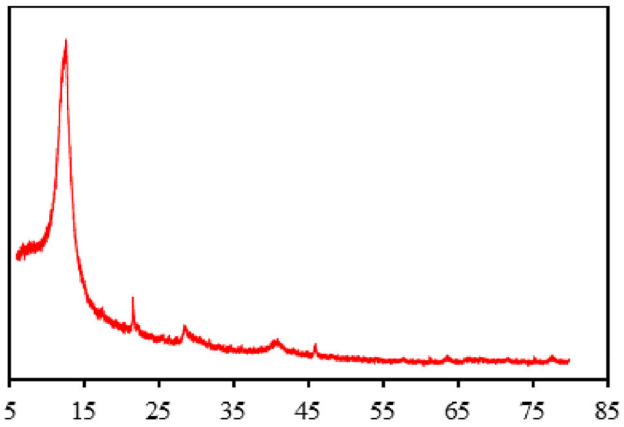

Figure 3. GO characterized by XRD analysis.

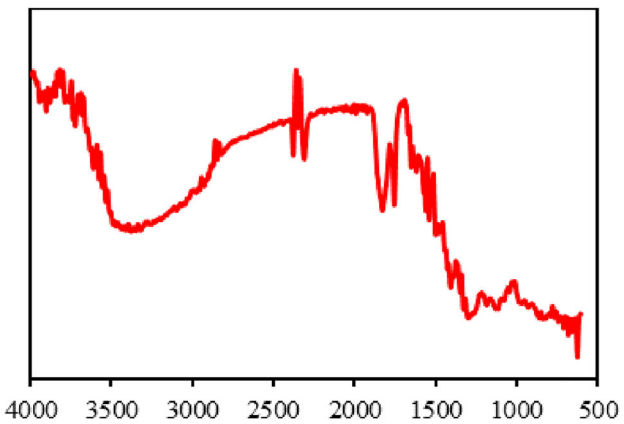

Figure 4. GO characterized by FTIR.

C39/C39M-18 at the curing period of 7 and 28 days using a 200-Ton compression testing machine. The load was applied gradually without shock at a rate of 250 ± 50 kPa s^{-1} until the load indication started to show a gradual decrease. The highest load taken by each specimen was noted, and an average value of three specimens was measured to calculate the compressive strength.

2.4 *Flexural strength*

In accordance with ASTM C78/C78M-22, the third point loading test for flexural strength was conducted on beams 100 × 100 × 500 mm on a universal testing machine for each curing age of 7 and 28 days. The specimen was positioned in the machine so that two points were used to

Table 2. Mix proportions of concrete per cubic metre.

Mix	GO (%*)	Fly ash (%*)	W/C ratio	Cement (kg)	Sand (kg)	CA (kg)	PCE (%*)
CC	0	0	0.30	450	800	1140	0.80
GC	0.15	0	0.30	450	800	1140	0.80
GFC10	0.15	10	0.30	450	800	1140	0.80
GFC20	0.15	20	0.30	450	800	1140	0.80
GFC30	0.15	30	0.30	450	800	1140	0.80

*Percentage by weight of cement.

apply the load to the top surface. The load was applied steadily at a rate between 0.9 and 1.2 N mm^{-2} min^{-1}. The highest load taken by each specimen was measured, and averages of three similar specimens were used.

2.5 *Stress–strain behaviour*

The stress–strain behaviours of concrete mixes under compression were evaluated by conducting a uniaxial compression test on a cylindrical specimen with dimensions of 100 mm diameter and 200 mm height. The load was applied monotonously without shock at a rate of 0.25 ± 0.05 MPa s^{-1}. Longitudinal deformations of a specimen in response to the applied load were measured with a data acquisition system connected to the load cell and LVDTs.

2.6 *Static modulus of elasticity*

Static modulus of elasticity was measured in accordance with ASTM C469-14. This test method is meant for the evaluation of elastic chord modulus of moulded concrete cylinders subjected to longitudinal compressive stress. Elastic chord modulus has been calculated from the ratio of the change in compressive stress and longitudinal strain at two points on the stress–strain curves. The first point is when the longitudinal strain is 0.000050 mm mm^{-1} and the second point is when the load is 40% of the ultimate load. The average of three specimens was considered to calculate the modulus of elasticity.

2.7 *Microstructure of concrete*

SEM is a super sophisticated and precise analytical technology that uses electron beams to generate magnified surface images of the preferred location. The produced raster scan image can have a resolution greater than 1 nm. Upon performing the compressive strength test, the sample was ground into smaller parts before being evaluated for SEM examination. The specimens were then properly cleaned and oven-dried at 60°C. Before SEM imaging, samples were sputter-coated with a thin coating of gold-palladium by means of a sputter deposition technique. Following that, the samples were examined using Tescan, Vega 3 LMU. This analytical technique is used to examine the sample's surface morphology. EDS is an analytical technique that is used to determine the elemental composition of various elements. The EDS method is based on the interaction of an X-ray excitation source and a sample.

2.8 *Numerical modelling*

The non-linear numerical modelling has been carried out using a finite element software. ATENA-GiD software was used in the present investigation for simulating the stress–strain behaviour of GO and fly ash-based concrete. For geometric modelling, GiD is an interactive tool that also serves as the data input for ATENA analysis. The material properties considered in the modelling were taken from the experimental results. GO and fly ash-based concrete behaviour was modelled as nonlinear under uniaxial stress.

3. Result and discussions

3.1 *Strength properties*

The values of compressive and flexural strength at 7 and 28 days for all concrete mixes are shown in figures 5 and 6.

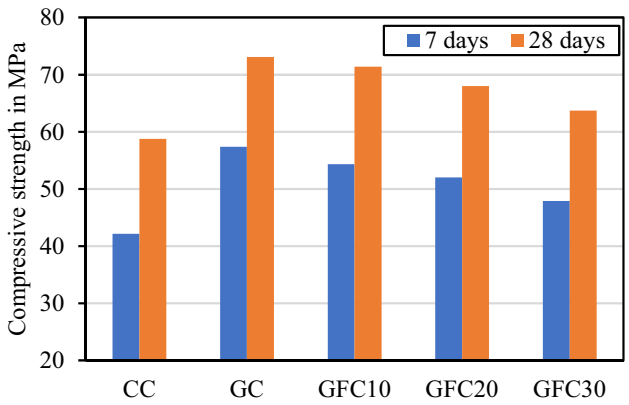

Figure 5. Compressive strength of concrete mixes.

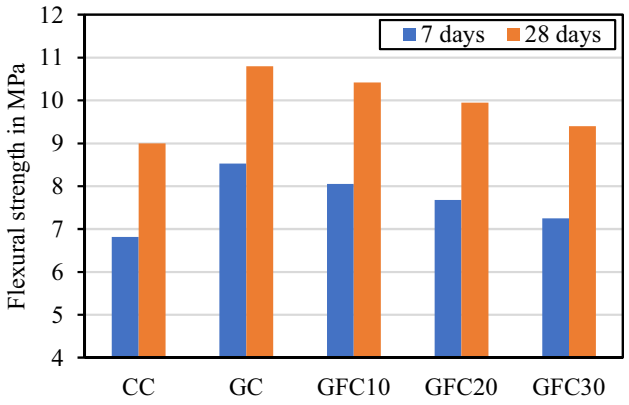

Figure 6. Flexural strength of concrete mixes.

The result shows that adding GO to concrete improved the compressive and flexural strength. These findings are consistent with relevant research [23–26]. The compressive and flexural strength of the GC mix was improved by 36 and 20% in comparison with the CC mix, respectively. The improvement in strength may be attributable to the improved mechanical interlocking owing to the wrinkled morphology of GO sheets, strong interaction between GONPs and cracks because of the high aspect ratio and 2-dimensional sheet-like structure [23,24]. It can also be ascribed to the reduction of the pore structure, acceleration of the hydration process and development of strong interfacial forces consequential from chemical interactions among oxygen functionalities and hydrated phases [23,24]. All the strength properties of these mixes diminished with the fly ash replacement compared to the GC mix. However, the compressive strength of specimens with the combination of GO and fly ash is greater than the CC mix. The compressive strength of the GFC mixes with fly ash replacements at 10, 20 and 30 percentages was enhanced by 28.9, 23.4 and 13.6% at 7 days, and 21.4, 15.6 and 8.4% at 28 days, respectively, compared to CC mix. Flexural strength of the GFC mixes with fly ash replacements at 10, 20 and 30 percentages was enhanced by 18.1, 12.7 and 6.4% at 7 days, and 15.8, 10.6 and 4.4% at 28 days, respectively, compared to CC mix. However, the strength properties of GFC mixes are less compared to GC mixes. The reason for this may be due to the fly ash replacement, fly ash has the disadvantage of delaying early stage strength improvement. The increase in strength properties of GFC mixes compared to the CC mix could be because of GO addition. It is observed that GO can compensate for the strength delay caused by fly ash [29]. The development in strength properties of GFC mixes may be due to the addition of GO and fly ash replacement, which improves the workability of fresh concrete composite and decreases the detrimental pore of hardened concrete composite, resulting in the increased strength properties of cement composite [29].

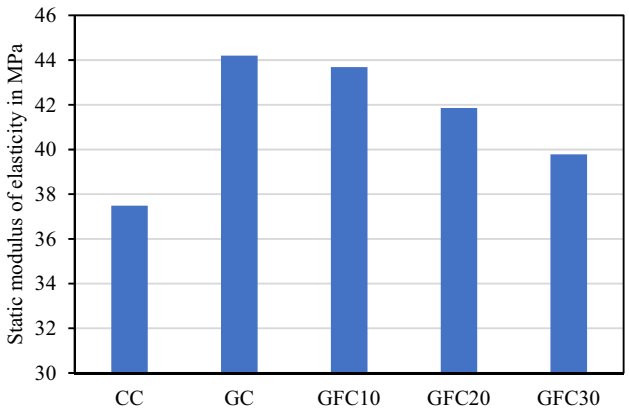

Figure 8. Static modulus of elasticity of all concrete mixes.

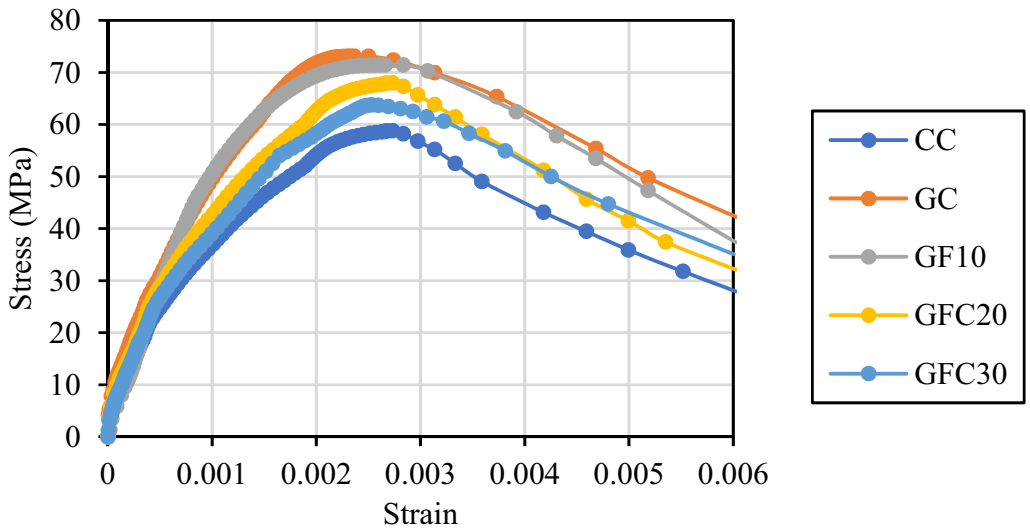

Figure 7. Stress–strain curves of all concrete mixes.

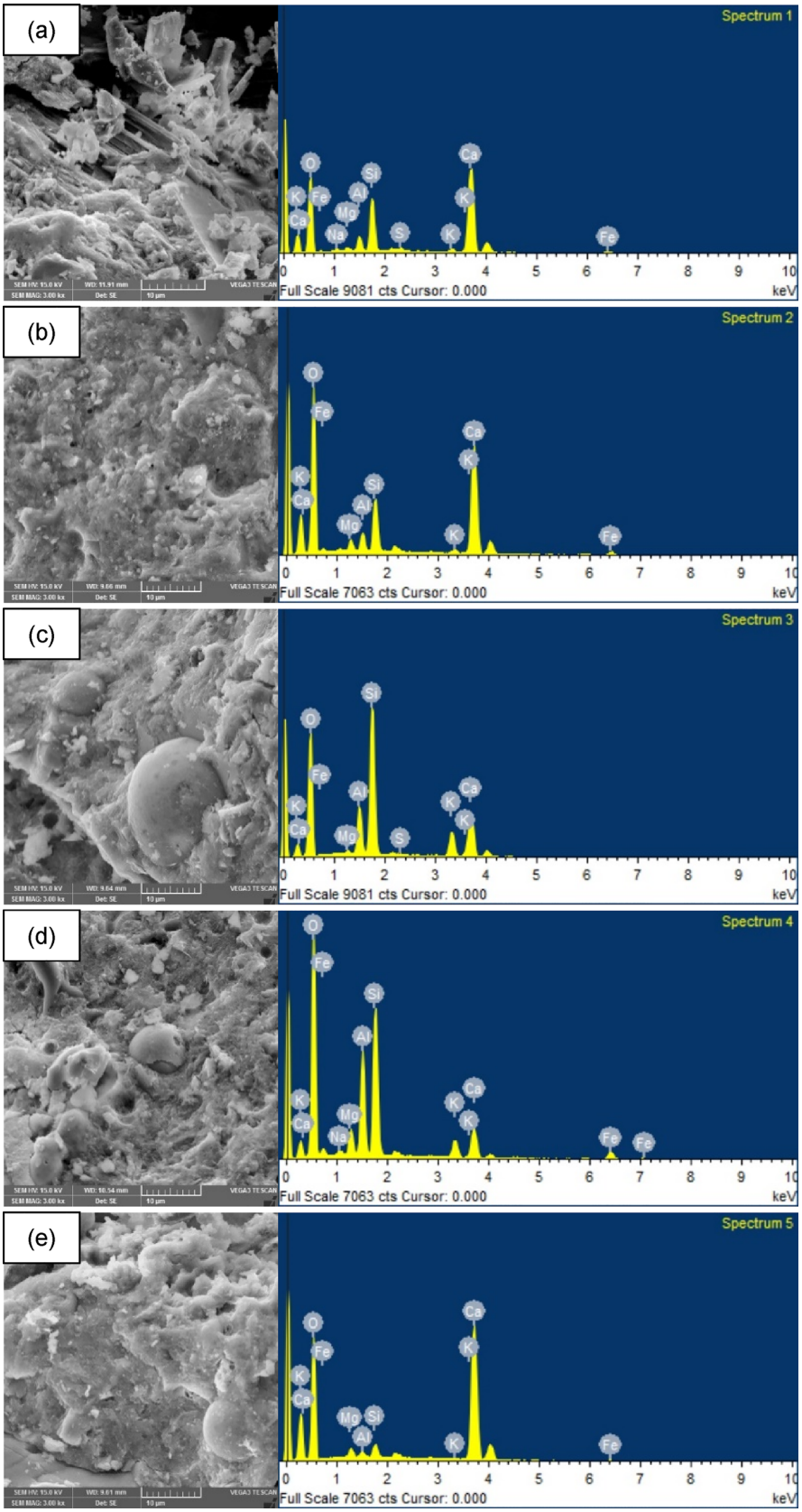

Figure 9. SEM and EDS of various concrete mixes: (**a**) CC, (**b**) GC, (**c**) GFC10, (**d**) GFC20, (**e**) GFC30.

Table 3. EDS analysis of various concrete mixes.

Mix	Weight percentage (wt%)								
	C	O	Al	Si	S	K	Ca	Fe	Mg
CC	4.29	56.67	3.86	4.42	2.22	1.54	23.80	1.42	1.36
GC	10.56	47.15	1.74	8.75	0.64	0.88	27.47	1.59	0.95
GFC10	10.09	45.15	2.13	8.54	0.55	0.68	29.48	2.45	0.57
GFC20	6.32	55.84	1.81	5.61	0.68	1.45	24.17	2.41	1.41
GFC30	5.13	58.25	2.72	5.21	1.04	1.26	23.77	1.05	1.25

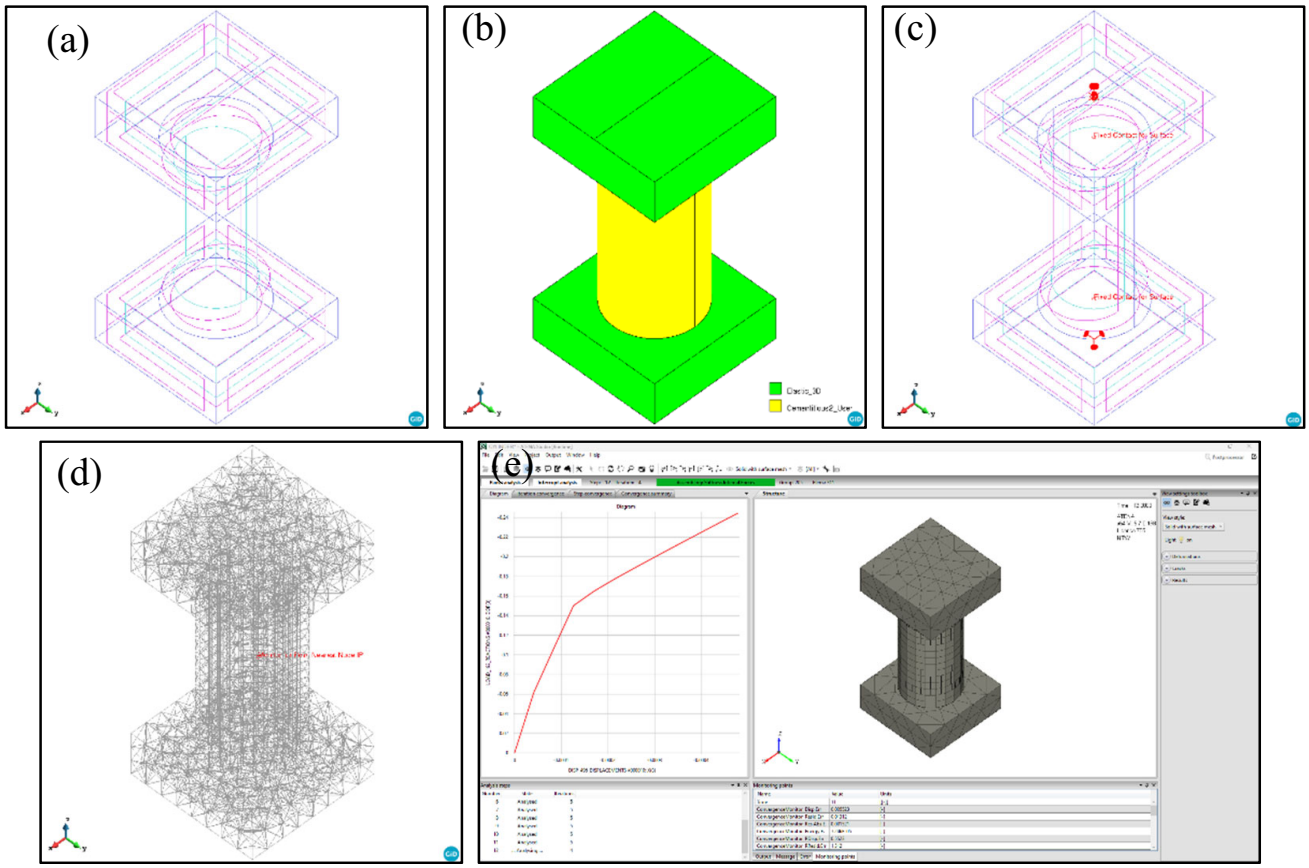

Figure 10. Modelling steps followed in ATENA-GiD software for cylinder. (**a**) Geometric model, (**b**) boundary conditions, (**c**) material properties, (**d**) meshing properties and (**e**) ATENA analysis.

3.2 *Stress–strain behaviour*

The stress–strain curves under uniaxial compression for all concrete mixes are presented in figure 7. Each curve is representative of three similar cylinders tested under compression at the age of 28 days. The parameters that can be determined from the stress–strain plots are the strain at maximum stress and the ultimate strain. It is observed from the stress–strain curves that the incorporation of GO enhanced the area under pre-peak portion owing to increased peak stress. While loading, nano-size cracks generate and develop as a continuous microcrack before reaching peak stress in the ascending portion of stress–strain curve [28]. The enhanced strain values indicate that presence of GO delays the initiation of microcrack propagation [28,29]. It can also be found that stress–strain behaviour of the concrete mixes with the partial replacement of fly ash is different due to variations in their compressive strength. The GFC10 concrete mix having percentages of fly ash at 10% shows the strain value at the peak stress similar to the GC concrete mix. Whereas, the GFC20 mix that had lower compressive strength compared to GC concrete showed a strain value at the peak stress which is slightly lower than the strain in GC concrete. On the other hand, the GFC30 mix that has overall lower compressive strength compared to GC concrete experienced lower values of strains

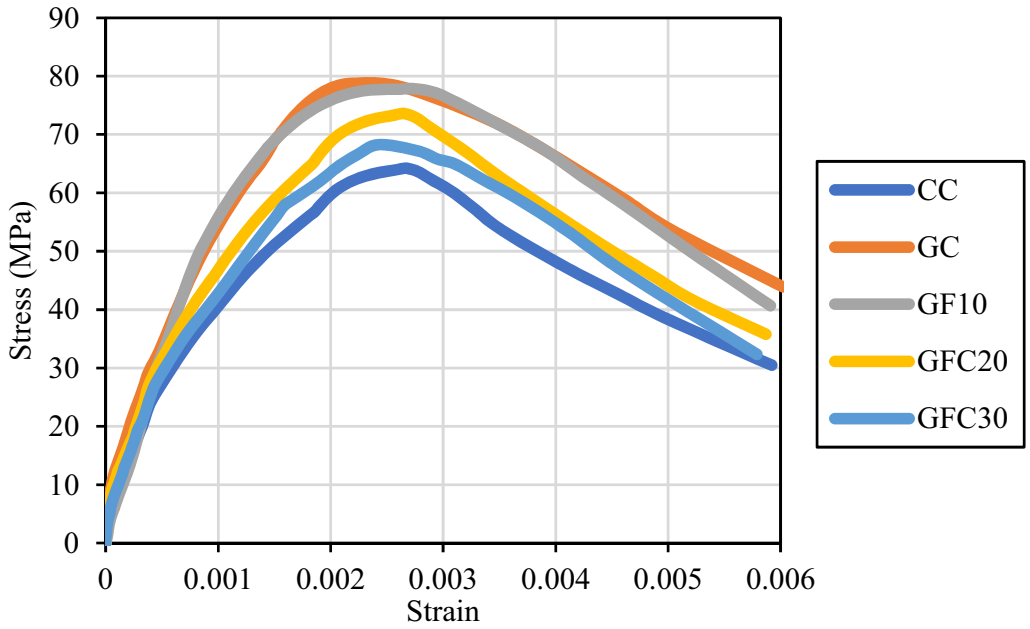

Figure 11. Stress–strain curves of all concrete mixes generated by ATENA model.

Table 4. Comparison of the peak stress from the experimental and numerical model.

Mix ID	Experimental	ATENA	% Error
CC	58.8	64.19	9.17
GC	73.1	78.82	7.82
GFC10	71.4	77.78	8.94
GFC20	68	73.58	8.21
GFC30	63.75	68.28	7.11

compared to GFC10 and GFC20. In contrast, all three mixes GFC10, GFC20 and GFC30 showed the strain at the peak stress is greater than the control concrete. Overall, it is concluded that a lower percentage replacement of cement with fly ash along with addition of GO exhibits an increased peak stress and corresponding strain compared to the control concrete.

3.3 *Static modulus of elasticity*

The static modulus of elasticity is taken as the tangent to the stress–strain curve under compression for all concrete mixes, is shown in figure 8. In general, stiffness and volume of constituents have the greatest influence on the elastic modulus of composites. As the dosage of GO in the concrete is only 0.15% by weight fraction, it can be observed that the modulus of elasticity of concrete with the incorporation of GO was greater than control concrete. The improvement in static elastic modulus could be attributed to a reduction in the number of original shrinkage cracks due to the prevention of microcracks by GO [24,29]. It can also be found in figure 8, the elastic modulus of the concrete mixes with fly ash replacement, such as GFC10, GFC20 and GFC30, showed an improvement compared to the CC mix. The improvement was higher when a lower percentage of cement was replaced with fly ash. In contrast, concrete mixes containing fly ash and GO exhibited less modulus of elasticity compared to the GC mix. These results are similar to the behaviour of compressive strength results. This result demonstrates that inclusion of GO and replacement of fly ash at lower percentage exhibits improved static elastic modulus compared to control concrete.

3.4 *Microstructure of concrete*

SEM images of the various concrete mixes with the addition of GO and varying fly ash replacements are shown in figure 9. The surface morphology of the CC mix is depicted in figure 9a. It can be seen that the formation of microcracks and pores in CH, C–S–H, Afm and Aft results in a loose and irregular structure. Figure 9b shows an SEM image of a GC mix sample, which clearly shows that, after adding GO to concrete, the crystalline phase of the hydrated products is densely intertwined with each other, with fewer pores and microcracks. When compared to the CC mix, the morphology of the GC mix sample demonstrates the development of a homogenous, and dense structure at the micro-level, which is accountable for the improvement of mechanical characteristics. GFC mix sample SEM images are depicted in figure 9c–e, and with the addition of fly ash

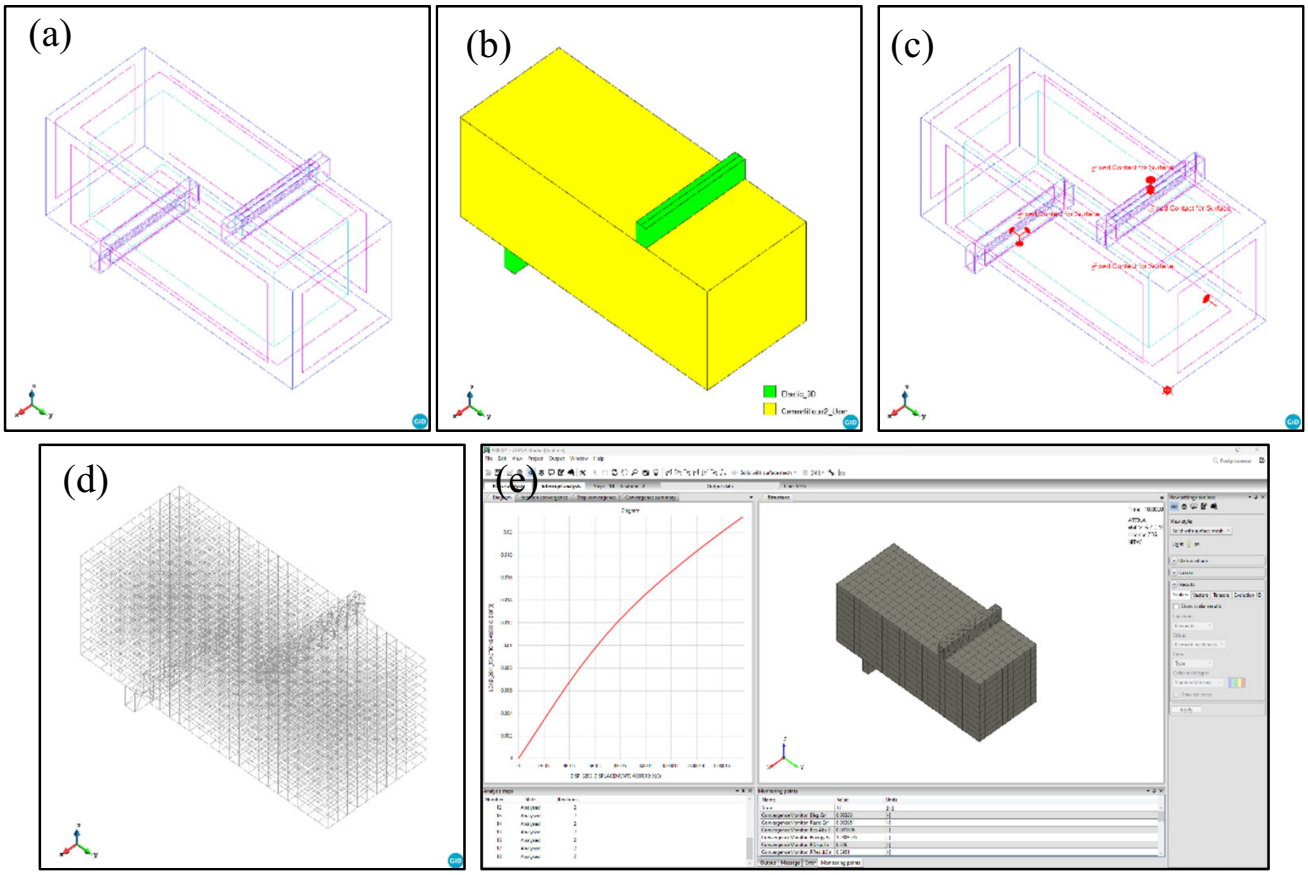

Figure 12. Modelling steps followed in ATENA-GiD software for prism. (**a**) Geometric model, (**b**) boundary conditions, (**c**) material properties, (**d**) meshing properties and (**e**) ATENA analysis.

Table 5. Comparison of the flexural strength from the experimental and numerical modelling.

Mix ID	Experimental	ATENA	% Error
CC	9.01	9.68	7.44
GC	10.8	11.28	4.44
GFC10	10.42	11.06	6.14
GFC20	9.95	10.55	6.03
GFC30	9.41	9.97	5.95

and GO, the structure of the cement hydration phases was strengthened over the CC mix sample. Unreacted fly ash particles of spherical shape were also seen, indicating that fly ash secondary hydration is progressing as the growth rate of strength characteristics of GFC mixes improved.

In order to investigate the elemental composition of the hydrated phases represented in the SEM images, an EDS analysis was carried out. Figure 9 depicts the spectrum 1–5, while table 3 gives the percentage composition of elements. Elemental analysis reveals that compared to the CC mix, the percentages of Ca, Si and C were much higher in the GC mix, while the amount of O was significantly lower. The elemental ratio of Ca/Si was quite high in the CC mix; however, this ratio was lowered when GO was incorporated into the mix. This demonstrates that mechanical properties are improved as a result of accelerated hydration in the presence of GO attributable to the formation of dense C–S–H structure and other interconnected hydrated phases [30].

4. Numerical modelling

ATENA-GiD software is a finite element-based program developed specifically for the nonlinear analysis of concrete elements. It required a lot of mixes and trials for the tedious experimental procedures, which take time and effort, to create a GFC concrete. A nonlinear model was developed with the use of the ATENA-GiD software, and it was then verified by experimental results.

4.1 *Compression modelling of a cylinder*

A cylindrical model was created using ATENA-GiD. The experimental findings of compressive strength and stress–strain results were used as input parameters. To estimate the stress–strain behaviour under compression, a cylindrical specimen having a size of 100 mm diameter and 200 mm

height was analysed to confirm the accuracy of the model, and then a flexure specimen with dimensions of 100 × 100 × 500 mm prismatic beam was analysed for validation in ATENA-GiD software. The element used in creating the model is a hexahedron for concrete specimens and a tetrahedron for supporting steel plates. The boundary conditions employed in this study were identical to those used in the analysis of the simply supported beam. Figure 10 shows the steps followed in modelling the 100 × 200 mm cylindrical specimen. Figure 11 shows the stress–strain behaviour from the FEM model using ATENA under uniaxial compression. Table 4 shows the findings of peak stress from the experimental and FEM model. The results obtained from the model using ATENA software are higher side compared to the experimental findings. It is also found that the results generated by the FEM model are in good agreement with experimental values, the percentage error in peak–stress is considerably less than 10%.

4.2 *Flexure modelling of a prismatic beam*

A flexural model of a prismatic beam of size 100 × 100 × 500 mm was modelled to validate the results obtained with experimental data and the values determined from the numerical modelling under flexure. Since the model considered for flexure is symmetric about the centre of the specimen, only half of it was examined and analysed with ATENA. Figure 12 depicts the steps involved in developing a model under flexure. The experimental concrete stress–strain curve under uniaxial loading is manually provided to create a numerical model under flexure. Table 5 demonstrates a comparison of the flexural strength obtained through numerical modelling and experimental study. The predicted flexural strength results are in good agreement with experimental values. The margin of error is less than 10%.

5. Conclusions

This investigation has presented an experimental and numerical study on the constitutive stress–strain behaviour of GO and fly ash-based high-strength concrete. The results presented include the strength properties, stress–strain behaviour and static elastic modulus. Based on the findings of this study, the replacement of cement with fly ash in concrete along with the addition of GO at a fixed dosage of 0.15% significantly influences the mechanical characteristics. The increased percentage of cement replacement with fly ash exhibited a decreasing trend in the mechanical characteristics; however, the final mechanical properties up to 30% replacement with fly ash were greater than control concrete. Also, the microstructure properties indicated that the concrete mixes with GO and fly ash exhibited a denser microstructure. The results obtained from the nonlinear numerical model were well agreed with the experimental findings with a percentage error of less than 10%. This investigation shows the feasibility of developing high-strength concrete using GO and fly ash. Further, the study demonstrates the creation of a numerical model using ATENA-Gid to avoid cumbersome experimental tests.

References

[1] Konsta-Gdoutos M S, Metaxa Z S and Shah S P 2010 *Cem. Concr. Compos.* **32** 110
[2] Jo B W, Kim C H, Tae G H and Park J B 2007 *Constr. Build. Mater.* **21** 1351
[3] Senff L, Labrincha J A, Ferreira V M, Hotza D and Repette W L 2009 *Constr. Build. Mater.* **23** 2487
[4] Sanchez F and Sobolev K 2010 *Constr. Build. Mater.* **24** 2060
[5] Agrawal S, Raghuveer M S, Ram P R and Ramanath G 2007 *IEEE Trans. Nanotechnol.* **6** 722
[6] Salvetat J P, Bonard J M, Thomson N H, Kulik A J, Forró L and Benoit W 1999 *Appl. Phys. A: Mater. Sci. Process.* **69** 255
[7] Liu G, Zhang H, Kan D, Tang S and Chen Z 2022 *Fuller. Nanotub. Carbon Nanostr.* **30** 1252
[8] Konsta-Gdoutos M S, Metaxa Z S and Shah S P 2010 *Cem. Concr. Res.* **40** 1052
[9] Cwirzen A 2010 *Adv. Mat. Res.* **123** 639
[10] Rafiee M A, Lu W, Thomas A V, Zandiatashbar A, Rafiee J and Tour J M 2010 *ACS Nano* **4** 7415
[11] Rafiee M A, Rafiee J, Wang Z, Song H, Yu Z-Z and Koratkar N 2009 *ACS Nano* **3** 3884
[12] Kuilla T, Bhadra S, Yao D, Kim N H, Bose S and Lee J H 2010 *Prog. Polym. Sci.* **35** 1350
[13] Lambert T N, Chavez C A, Lu P, Bell N S and Ambrosini A 2009 *J. Phys. Chem. C* **113** 19812
[14] Cao Y, Zhang J, Feng J and Wu P 2011 *ACS Nano* **5** 5920
[15] Kim J, Cote L J, Kim F, Yuan W, Shull K R and Huang J 2010 *J. Am. Chem. Soc.* **132** 8180
[16] Reddy P V R K and Prasad D R (2022) *Jordan. J. Civ. Eng.* **16** 507
[17] Reddy P V R K and Ravi Prasad D (2022) *Mater. Today Proc.* **62** 2919
[18] Avanish P S, Monika M, Amita C and Dhawan S K 2011 *Nanotechnology* **22** 465701
[19] Xu Z and Gao C 2011 *ACS Nano* **5** 2908
[20] Reddy P V R K, Ravi Prasad D (2024) *Bull. Mater. Sci.* **47**(1). https://doi.org/10.1007/s12034-023-03092-1
[21] Li G Y, Wang P M and Zhao X 2005 *Carbon* **43** 1239
[22] Chintalapudi K and Pannem R M R 2022 *Fuller. Nanotub. Carbon Nanostr.* **30** 987
[23] Reddy P V R K and Prasad D R 2022 *J. Build. Pathol. Rehabil.* **7** 30
[24] Reddy P V R K and Prasad D R 2023 *J. Build. Eng.* **63** 105481
[25] Yuan X and Liao G 2023 *Fuller. Nanotub. Carbon. Nanostr.* **31** 51
[26] Reddy P V R K and Prasad D R 2023 *Fuller. Nanotub. Carbon Nanostr.* **31** 255

[27] Reddy P V R K and Ravi Prasad D (2024) *Fullerenes Nanotubes and Carbon Nanostructures* **32(4)** 380–388 https://doi.org/10.1080/1536383X.2023.2287603

[28] Wang Q, Cui X, Wang J, Li S, Lv C and Dong Y 2017 *Constr. Build. Mater.* **139** 35

[29] Reddy P V R K and Prasad D R 2024 *Lecture Notes in Civil Engineering* **440** 421–431 https://doi.org/10.1007/978-981-99-7464-1_31

[30] Kunther W, Ferreiro S and Skibsted J 2017 *J. Mater. Chem. A* **5** 17401